Journal of Magnetic Resonance **150,** 26–34 (2001)
doi:10.1006/jmre.2001.2315, available online at http://www.idealibrary.com on IDEAL®

A Time-Resolved EPR Study of the Electron-Spin-Polarization Pathways of *p*-Benzosemiquinone

Martin Jäger and James R. Norris, Jr.[1]

Department of Chemistry, University of Chicago, 5735 South Ellis Avenue, Chicago, Illinois 60637

Received October 2, 2000; revised January 23, 2001; published online April 17, 2001

Benzoquinone (BQ), deuterobenzoquinone (d_4-BQ), and hydroquinone (BQH_2) are investigated in ethylene glycol by means of direct detection fast time-resolved EPR spectroscopy after laser flash photolysis. The development of the magnetization as a function of time and magnetic field is obtained and analyzed in terms of the Bloch equations and hyperfine parameters. The signals are attributed to the semiquinones $BQH^\bullet$ and d_4-$BQH^\bullet$. The presence of 1,2-dihydroxyethyl radicals during the photolysis of BQ and d_4-BQ is verified. No alkyl radicals are observed in solutions of BQ with excess BQH_2. Detailed analysis of the chemically induced dynamic electron polarization spectra with respect to their development in time shows that polarization patterns of the semiquinones can be traced back to a superposition of triplet mechanism and radical pair mechanism, the latter arising from geminate T-pairs. Hence, two independent pathways for polarization are assumed: reaction of triplet benzoquinone with ethylene glycol leads to the semiquinone and dihydroxyethyl radicals with all signals in emission, whereas the reaction of triplet BQ and BQH_2 yields two semiquinones exhibiting both net emissive and multiplet emissive/absorptive intensity distributions.

Key Words: **time–resolved EPR; CIDEP; triplet mechanism; radical-pair mechanism; photochemistry.**

INTRODUCTION

The exploration of chemically induced dynamic electron polarization (CIDEP) has become inseparable with time-resolved electron paramagnetic resonance (TREPR) spectroscopy (*1*). Among TREPR techniques, "direct detection," i.e., continuous wave EPR without field modulation, which records the time- and field-dependent signals of radicals generated by flash photolysis or pulse radiolysis, is established as among the most powerful tools for the investigation of submicrosecond lived paramagnetic intermediates (*2–4*). *Para*-benzoquinone (BQ), among the first photochemically reactive systems observed to exhibit CIDEP, has been intensely studied with respect to its light-induced reaction pathways. The influence of reaction conditions, such as pH, temperature, solvent polarity, viscosity, and flow rates, has led to different views of the chemical and physical processes (*5–9*).

The intention here is to explore further the magnetic resonance properties of BQ by applying fast time-resolved continuous-wave EPR to monitor the transient magnetization signals of BQ and of deutero-benzoquinone (d_4-BQ) as a function of external magnetic field. A complete spectral analysis based upon a Bloch equation treatment is performed for BQ and d_4-BQ radicals with respect to the triplet and radical pair mechanism (TM, RPM) of CIDEP. The EPR signal of the ethylene glycol radical is detected and an estimate of its lifetime is given. The origin of the RPM is discussed in terms of viscosity, concentration, photoreaction pathways of BQ, and experimental conditions. Results are compared to earlier observations reported in the literature.

THEORY

The development of the magnetization $\mathbf{M}(t)$ in a magnetic field along the z-axis is described by the Bloch Eq. [1], where $\mathbf{L}$ is the relaxation matrix containing the longitudinal and transversal relaxation times T_1 and T_2, the microwave field strength ω_1, the offset of the magnetic field from resonance $\Delta\omega$, the number of radicals n in the sample, and the magnetization and polarization at thermal equilibrium $\mathbf{M}_{\text{eq}}$ and P_{eq},

$$\frac{d}{dt}\mathbf{M} = \underline{\underline{\mathbf{L}}}\mathbf{M}(t) + \frac{1}{T_1}\mathbf{M}_{\text{eq}}, \qquad [1]$$

where

$$\underline{\underline{\mathbf{L}}} = \begin{pmatrix} -\frac{1}{T_2} & \Delta\omega & 0 \\ -\Delta\omega & -\frac{1}{T_2} & \omega_1 \\ 0 & -\omega_1 & -\frac{1}{T_1} \end{pmatrix}, \quad \mathbf{M}(t) = \begin{pmatrix} M_x(t) \\ M_y(t) \\ M_z(t) \end{pmatrix},$$

$$\mathbf{M}_{\text{eq}} = n P_{\text{eq}} \begin{pmatrix} 0 \\ 0 \\ 1 \end{pmatrix}.$$

As is the general procedure for flash photolysis experiments (*7*), the generation of radicals and thus the creation of

[1] Member of the Institute for Biophysical Dynamics.

1090-7807/01 $35.00

polarization are assumed complete before observation. Also neglected is F-pair polarization, which occurs outside the observation period of short response time detection ($t_{res} \ll T_1$), where no magnetic field modulation is applied and the development of the *y*-component of the magnetization as a function of time is the considered experimental quantity. Contributions from initial and equilibrium polarization (referred to as P_i and P_{eq}) can thus be separated according to the general solution [2] for Eq. [1].

$$M_y(t) = n(t)[P_i g_y(t) + P_{eq} G_y(t)] \quad [2]$$

The derivation, solution, and analysis of the eigenvalue problem have been extensively discussed elsewhere (*10*, *11*). The function $g_y(t)$ is known to be of form [3], e.g.,

$$g_y(t) = \sum_{i=1}^{3} A_{iy} \exp(\lambda_i t), \quad [3]$$

with λ_i as the eigenvalues of $\underline{\underline{\mathbf{L}}}$ and the coefficients A_{iy}

$$A_{1y} = \frac{\omega_1\left(\lambda_1 + \frac{1}{T_2}\right)}{(\lambda_1 - \lambda_2)(\lambda_1 - \lambda_3)},$$

where A_{2y}, A_{3y} can be obtained by cyclic permutation of the indices i of λ. The radical concentration is given by Eqs. [4] or [5] when the radical decay follows a first- or second-order decay, k_1 and k_2 being the appropriate rate constants.

$$n(t) = n(0)\exp(-k_1 t) \quad [4]$$

$$n(t) = n(0)[1 + k_2 n(0) t]^{-1} \quad [5]$$

From the different possible pathways that lead to polarized signals such as the triplet, radical pair, radical triplet pair, and spin correlated radical pair mechanisms, only TM and RPM were found to be active in the course of this investigation. As no attention is paid to the absolute magnitude of the contributions, the initial polarization caused by the TM was arbitrarily set to unity for all lines. In contrast, the RPM leads to P_i according to Eqs. [6] and [7].

$$P_i \sim \sqrt{\frac{Qd^2}{D}} \quad [6]$$

$$Q_{ab} = \frac{1}{2}\Delta g \mu_B B + \frac{1}{2}\sum_n a_{1n} m_{1n}^{(a)} - \frac{1}{2}\sum_m a_{2m} m_{2m}^{(b)}, \quad [7]$$

where D is the diffusion rate, d the distance of closest approach, and a_{1n} the hyperfine coupling constant of nucleus n on radical 1 in the overall nuclear spin state a. All other symbols have their usual meanings. Full derivations and extensive discussions have been given previously (*12*, *13*).

In order to calculate the field dependence of transient signals, a stick spectrum, representing resolved hyperfine interactions, is simulated by systematic variation of the off-resonance frequencies $\Delta\omega$ for all hyperfine lines. The resulting intensities are subsequently added. To account for unresolved hyperfine structure ($a > \omega_1$), the simulation is convoluted with a Gaussian lineshape function.

The observed signal may be decomposed into a sum of contributions from mechanisms treated as independent (*14*). This seems justified here, as the polarization is established before observation; furthermore, each mechanism invoked below induces nonequilibrium spin populations in a certain fraction of molecules. The resulting signals corresponding to each fraction are eventually superimposed. The special case described in this paper where two radical generation pathways lead to the same reaction product renders this distinction necessary.

EXPERIMENTAL

The spectrometer consists of a Varian E-Line based magnet and field controller, equipped with a personal computer for automation. The field is measured independently with a Bruker ER 035 M gaussmeter. A Bruker microwave bridge ER 041 MR has been modified to enhance time resolution and increase sensitivity. The raw signal is amplified with a Hewlett–Packard 461A and directed into either a LeCroy 9450 dual oscilloscope when recording time traces at various field positions or an EG&G PAR 162 boxcar averager when field scanning at a constant time period is desired. The data are finally stored into the personal computer. A Varian V-Line optical transmission cavity is used to minimize the laser-light-induced background signal and to improve the time resolution by lowering the *Q*-factor compared to the standard Varian TE_{102} cavity. The samples are flowed through a suprasil quartz flat cell. The flow rate was sufficiently fast that each laser flash excited fresh solution. A Lambda Physik excimer laser EMG 103 MSC, operated at $\lambda = 308$ nm, 20- to 100-Hz repetition rate, ~10–20 mJ/ pulse at the sample, and 15- to 20-ns pulse width, serves as light source. Synchronization with the signal recorder is achieved via a fast photodiode or the synchronous output channel of the laser. The EPR signal rise time was determined to be 20–30 ns.

Ethylene glycol was purchased from Fisher and d_4-benzoquinone from Aldrich and were used without further purification. Benzoquinone was obtained from Acros and purified according to standard methods (*15*) prior to use.

RESULTS

1. Benzoquinone

The observation of the transient signals of BQ in ethylene glycol at low incident microwave power (~0.6 mW) yields the 3-dimensional surface shown in Fig. 1a when the field is varied in steps of 0.01 mT. The EPR spectrum, given in Fig. 1b

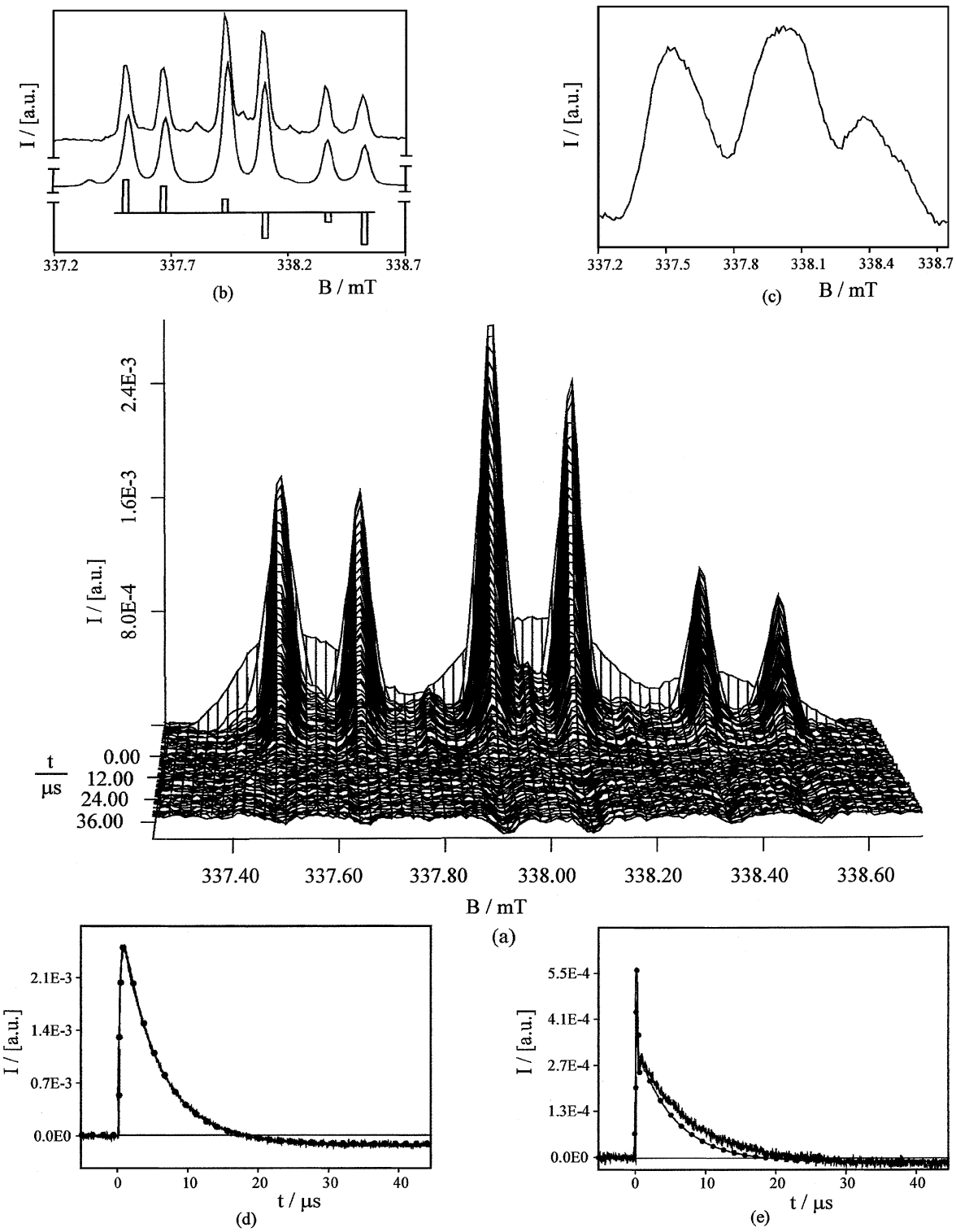

FIG. 1. (a) Signal of BQH$^\bullet$ (0.01 M) in ethylene glycol as a function of time and magnetic field after laser excitation at 308 nm, $\omega_1/2\pi = 4.1$ kHz. (b) Field domain spectrum of BQH$^\bullet$ at $\tau = 250$ ns, experimental (top), simulated with a Gaussian linewidth of 0.032 mT (middle), and stick plot of intensity distribution due to the RPM according to Eq. [10] (bottom). (c) Field domain spectrum of BQH$^\bullet$ at $\tau = 100$ ns. (d) Time domain signal of BQH$^\bullet$ at the first highfield hyperfine line (on-resonance), experimental (solid) and calculated (dotted). (e) Time domain signal of BQH$^\bullet$ off-resonance by $\Delta\omega = -0.04$ mT from the first highfield hyperfine line, experimental (solid) and calculated (dotted).

TABLE I
Hyperfine Coupling Constants, *a*, *g*-Values, Relaxation Times T_1, T_2 of BQH•, d_4-BQH•, and HO–CH_2–C•H–OH

	Parameters					
Radical	a/mT	a/mT	a/mT	*g*-factor	T_1/μs	T_2/μs
BQH•	0.43(1) (2 H, *ortho*)	0.16(1) (1 H, OH)	—	2.00463(5)	5.4	0.3
d_4-BQH•	0.075(10) (2 D, *ortho*)	0.19(1) (1 H, OH)	—	2.00463(5)	2.2	0.9
$HO–CH_2^{\beta}–C^{\bullet}H^{\alpha}–OH^{\beta}$	1.77(1) (1 H, α)	1.02(1) (2 H, β)	0.11(1) (1 H, OH^{β})	2.00308(5)	0.6	0.4

at 250 ns after the laser flash, is readily interpreted in terms of the hyperfine parameters given for BQH• in Table 1. The *meta*-protons splittings remain unresolved. Additional physical rates, used for all calculations, are the diffusion constant $D = 3.9 \times 10^{-9}$ m^2 s^{-1} and the distance of closest approach $d = 4 \times 10^{-10}$ m (*7*). For all calculations, it is also assumed that the spin–lattice relaxation time is faster than the radical termination reactions. For better visualization in the figures, the emission lines are deliberately shown above the baseline throughout this work in contrast to the conventional representation. Hence, all lines appear in emission at earlier times but change to absorption after about 18 μs. The deviation of the six-line spectrum from a 1 : 1 : 2 : 2: 1: 1 intensity pattern expected for both TM polarized and equilibrated signals is obvious. The imbalance of the lines is well fitted by superimposing TM and multiplet ($\Delta g = 0$) RPM polarized signals. Substituting the multiplet effect by a net effect ($\Delta g \neq 0$) does not lead to a comparable agreement. A second EPR spectrum for $\tau = 100$ ns is given in Fig. 1c. Strong line broadening decreases the spectral resolution, resulting in only three discernible lines. The weaker intensity of the high field part compared to the low field emission as a consequence of the RPM contribution can, however, already be recognized. Because of the low microwave field strength at the sample, oscillations in time and field are not yet observed, rendering the estimation of ω_1 and T_2 more difficult. Figure 1d presents the on-resonance time trace of the first high field hyperfine line (solid) in excellent agreement with the calculated one (dotted line). A decay off-resonance to this line by $\Delta\omega = -0.04$ mT is illustrated in Fig. 1e. Other lines show similar agreement between experimental and calculated time-dependent signals.

2. Deutero-(d_4)-benzoquinone

A 3-D surface of d_4-BQ was recorded at 50-mW incident microwave power over a range of 5.8 mT. The field domain spectrum at $\tau = 485$ ns is exemplarily shown in Fig. 2a (top). The corresponding calculation (bottom) is achieved by using the parameters given in Table 1 for d_4-BQH•. Again, a superposition of TM and RPM is found to contribute to the polarization. The transient of the first hyperfine line of the central signal (as indicated by the arrow) and its corresponding simulation are illustrated in Fig. 2b. Because of the higher microwave field strength, oscillations in the time domain are now observed, allowing a more exact determination of ω_1 and T_2. Due to a lower initial concentration of d_4-BQ (5×10^{-3} M), the signal-to-noise ratio is less favorable. A second radical species is present in the

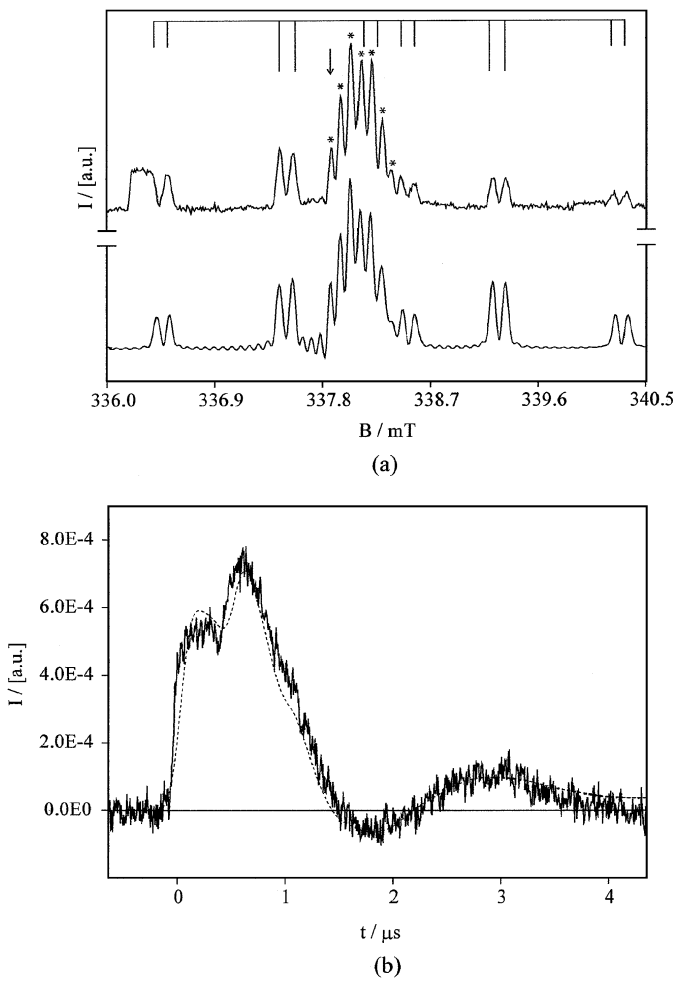

FIG. 2. (a) Field domain EPR spectrum obtained from a 3-D representation of the d_4-BQH• signal in ethylene glycol at $\tau = 485$ ns, $\omega_1/2\pi = 390$ kHz, experimental (top) and calculated (bottom), Gaussian linewidth 0.030 mT. Asterisks indicate signals corresponding to d_4-BQH•. The stick plot indicates 1,2-dihydroxyethyl radical emission lines. (b) Transient signal of d_4-BQH• observed at the magnetic field value of the first low field hyperfine line (on-resonance), indicated by the arrow in (a).

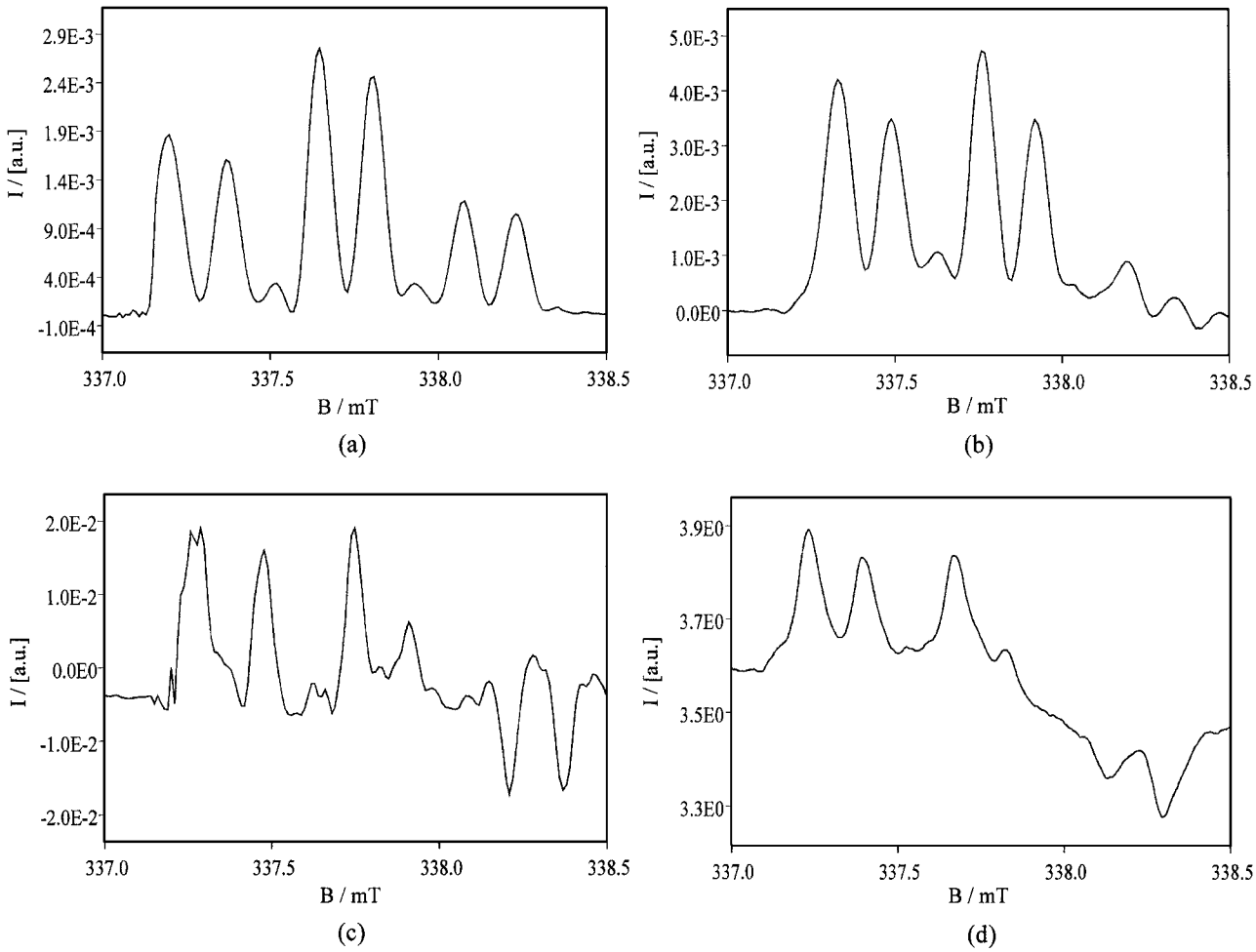

FIG. 3. Field domain EPR spectra of $BQH^{\bullet}$ in ethylene glycol containing the initial concentrations c_i: $c_i(BQ) = 0.02$ M at $\tau = 400$ ns, $\omega_1/2\pi = 390$ kHz. Experiment duration time and scan time: 4 h (a); $c(BQ) = 0.02$ M at $\tau = 400$ ns, $\omega_1/2\pi = 390$ kHz. Experiment duration time: 6 h preparation and 4 h scan time (b); $c_i(BQ) = 0.001$ M at $\tau = 1250$ ns, $\omega_1/2\pi = 390$ kHz. Experiment duration time: 4 h (c); $c_i(BQH_2) = 0.02$ M containing small amounts of BQ at $\tau = 1.5$ ns, $\omega_1/2\pi = 40$ kHz. Scan time: 200 s, integration time: 100 ns (d).

sample. The corresponding larger hyperfine components (indicated by the stick plot) are attributed to a hydroxyalkyl radical with parameters collected in Table 1. The signal decays with a rate constant of $\sim 0.5\ \mu$s. The broad signal in the low field region of the spectrum in Fig. 2a is believed to be caused by a random glitch in the microwave detector level.

3. Variation of Experimental Conditions

Figure 3 presents the EPR spectra of BQ after light excitation under various experimental conditions. Figures 3a and 3b originate from the same sample; the field domain spectra are taken from a 3-D surface at $\tau = 400$ ns of an experiment with 4 h duration (a) and another 4-h experiment starting 2 h later (b). Sample concentrations were 2×10^{-2} M. At lower concentrations (1×10^{-3} M), a field domain section at $\tau = 1250$ ns, as shown in Fig. 3c, can be observed. The high field part of the signal is clearly in absorption while the low field half remains in emission. The same pattern is recorded when scanning the field using boxcar integration but exciting a solution of hydroquinone containing small amounts of BQ, cf., Fig. 3d.

DISCUSSION

The transient EPR signals of BQ and d_4-BQ depending on field and time after laser excitation at 308 nm are well interpreted by applying the theory summarized in Eqs. [1] through [7] to the parameters given in Table 1. In accordance with earlier observations (*13*, *16*), the hyperfine (hf) parameters indicate the formation of the neutral semiquinone radical $BQH^{\bullet}$ (*17*). The perdeuterated species is found to yield d_4-$BQH^{\bullet}$. The observation of the hydroxyl proton splitting excludes hydrogen abstraction (or successive electron proton transfer) from the carbocyclic moiety of another benzoquinone molecule. By fitting the transient signals of $BQH^{\bullet}$ and d_4-$BQH^{\bullet}$, cf., Figs. 1d, 1e,

and 2b, the relaxation parameters collected in Table 1 are obtained. Previous estimates for $BQH^{\bullet}$ range from 2.3 to 7.8 μs for T_1, whereas only one value, 0.72 μs, is given for T_2 (*13*, *16*, *18*). No values for the deuterated benzoquinone are—to the best of our knowledge—reported in the literature. Hence, the parameters calculated within this work are found to be in good agreement with those estimated earlier. The variations in the relaxation times may arise from different experimental conditions. Influences on the relaxation parameters are due to temperature and viscosity of the solvent as well as to the oxygen concentration present in the sample. While the values obtained by Muus *et al.* (*16*) were obtained from power-dependent measurements of linewidths in the steady-state mode, parameters evaluated within the other works cited herein as well as this work are based on time-resolved experiments, which are usually carried out at higher initial benzoquinone concentrations. Furthermore, uncertainty in our estimations arises from the multiple parameter fittings carried out when simulating the complete 3-D surfaces. It may therefore be concluded that all measurements point toward the right order of magnitude, but the exact values will require correction for relaxation dependence on temperature, viscosity, and concentration of the compounds. The relaxation times of BQ and its deuterated isomer do not need to be identical. In addition, the experimental conditions applied in our experiments result in a smaller error in the estimation of T_1 for $BQH^{\bullet}$ than for d_4-$BQH^{\bullet}$, whereas T_2 is evaluated more exactly for the deuterated semiquinone. Attempts at improving the simulations were abandoned since calculations that included chemical exchange effects resulted in a slightly (10%) shorter longitudinal relaxation time for $BQH^{\bullet}$ but deteriorated the agreement between experimental and simulated transient signals.

Photochemistry of BQ is agreed (*19–22*) to proceed according to Eqs. [8] and [9],

$$BQ + h\nu \rightarrow BQ^{*} \rightarrow BQ^{T} \quad [8]$$

$$BQ^{T} + R\text{-}H \rightarrow BQH^{\bullet(P)} + R^{\bullet(P)}. \quad [9]$$

Because the polarized EPR signals of $BQH^{\bullet}$ and $R^{\bullet}$ are detected from the earliest time of the experiment, no distinction between hydrogen atom abstraction and electron transfer followed by proton transfer in reaction [9] is possible. As is exemplarily shown for d_4-BQ in Fig. 2a, but can also be observed for BQ, the signal of $R^{\bullet}$ (RH = ethylene glycol) is clearly recognizable. Its hf splitting constants are in good agreement with the ones of the dihydroxyethyl radical $HO\text{–}CH_2\text{–}C^{\bullet}H\text{–}OH$ reported previously (*23*); thus, the anticipated formation of the hydroxyalkyl radical as a result of reaction [9] is verified. Its lifetime, however, is much longer than assumed earlier ($\sim$10 ns (*13*)); the species is observable for a period of approximately 1.3 μs. The signal decay is dominated by a rate constant of 0.5 μs. Based on simulations, values of 0.6 and 0.4 μs are attributed to T_1 and T_2, respectively. However, since the hydroxyalkyl radical, a secondary radical, is not stable, the reaction rate might be of the same order of magnitude such that the decay would then reflect the radical termination or propagation rate. The polarization enhancement cannot be accurately determined within the chosen observation window, preventing distinction between primary and secondary rate of decay.

Before discussing the molecular origin of the RPM polarization, the nature of the effect must be considered. The observed intensity I_i of each hyperfine line i at a given time results from contributions of TM and RPM. Only in case of a multiplet effect ($\Delta g = 0$) is the RPM contribution to the overall spectral intensity $\sum_i I_i$ equal to zero. With the degeneracy n_i of the ith hyperfine line and the total degeneracy $N = \sum_i n_i$, the intensity of each line due to the multiplet effect can simply be calculated according to Eq. [10].

$$I_{i,\mathrm{RPM}} = I_i - \frac{1}{N}\sum_i n_i I_i \quad [10]$$

The resulting intensities based completely on experimentally obtained quantities are plotted in Fig. 1b. The pattern is in excellent agreement with that predicted for a multiplet effect. In addition, the change from emission to absorption in the spectral center is inconsistent with a net effect characterized by $\Delta g = 0.00155$.

When light modulation experiments with time resolution of the orders of hundreds of milliseconds were used for the investigation of $BQH^{\bullet}$, the deviation from the theoretical 1 : 1 : 2 : 2 : 1 : 1 intensity pattern expected for TM has been attributed to F-pair polarization[2] of similar radicals ($\Delta g = 0$), caused by the depletion reaction [11] (*7*, *13*, *16*).

$$2\ BQH^{\bullet(P)} \rightarrow BQ + BQH_2 \quad [11]$$

However, the E/A multiplet pattern can be recognized even at rather early times (100 ns) after the laser light pulse, as illustrated in Fig. 1b. It then decays without changing its ratio to the polarization created by TM. As a consequence, the superscript (P) in the case of BQH refers to both TM and RPM populations. Unfortunately, F-pairs and geminate pairs of triplet precursors (T-pairs) cannot be distinguished by means of their signal phases, as both are known to show the E/A pattern (*24*). Nevertheless, F-pair polarization must be excluded in this case because of the following observations:

(a) The contribution of the multiplet effect with respect to the TM-created polarization increases with decreasing initial benzoquinone concentration (cf. Figs. 3a and 3c), which in turn renders collisions from randomly diffusing radicals less frequent.

(b) The ratio of RPM to TM contributions depends on the viscosity of the solvent. The higher the viscosity, the more pronounced the multiplet effect. A strong multiplet effect is

[2] That is, polarization due to the reencounter of radicals after a period of free, independent diffusion.

observed in ethylene glycol, a weaker one in isopropanol, and no effect in ethanol or water. In contrast, F-pair polarization should be favored by lower viscosity solvents that cause an increase of the escape rate from the initial solvent cage.

(c) The RPM contribution is present at quite early times, whereas F-pair polarization is commonly observed at times $t \gg 5 \times T_1$; hence F-pair polarization is usually considered negligible in flash photolysis experiments (*25*).

The radical triplet pair mechanism, which might lead to a similar multiplet pattern superimposed onto a net emission (*26, 27*), has been excluded, as no signals of persistent free radicals have been detected in the sample, hence lacking the doublet precursor for the activation of that CIDEP mechanism.

Multiplet polarization can only arise from T-pairs if two semiquinone radicals fulfill the RPM conditions, i.e., a common creation, a period of level mixing while diffusing apart and spin rephasing by exchange interaction at a reencounter. As weak signals of the semiquinone anion are only present at times later than the appearance of the neutral semiquinone, multiplet polarization is most likely to result from the interaction of two $BQH^{\bullet}$. It is therefore straightforward to invoke the photochemical reaction between benzoquinone and hydroquinone (BQH_2) according to reaction [9] where RH now refers to BQH_2. It is easily realized that the so-formed $BQH^{\bullet}$ will carry both TM and RPM initiated polarization when EPR observation starts, provided the solvent viscosity is high enough to allow the reencounter. The proximity between BQ and BQH_2 required for the reaction to proceed is ensured by the formation of the quinhydrone complex (*28*). As a consequence of reaction [9] where RH can be a solvent or hydroquinone molecule, the semiquinone will exhibit a stronger overall signal than will the hydroxyethyl radical; the signal of the latter, however, is already less intense due to its shorter lifetime. After radical creation, the propagation and termination pathways of $BQH^{\bullet}$ follow Eqs. [11] to [15], where RH refers to ethylene glycol.

$$BQH^{\bullet} + BQ \rightarrow BQ + BQH^{\bullet} \quad [12]$$

$$R^{\bullet} + BQ \rightarrow BQ^{\bullet}\text{-}R \quad [13]$$

$$BQ^{\bullet}\text{-}R + BQ \rightarrow BQ\text{-}R + BQH^{\bullet} \quad [14]$$

$$2\,BQ^{\bullet}\text{-}R \rightarrow BQ\text{-}R + BQ + RH \quad [15]$$

Resulting from Eqs. [8], [9], and [11] to [15], two molecules of BQ are transformed into hydroquinone and an ethylene glycol adduct of the quinoid compound, labeled BQ-R. Thus, when recirculating the sample, the concentration of BQ in the solution decreases, whereas the amount of hydroquinone increases with experiment duration. The multiplet effect is therefore expected to become increasingly pronounced with time. This is illustrated in Figs. 3a and 3b, where spectra are taken at $\tau = 400$ ns after the laser pulse within 4 and 10 h experiment duration, respectively. Furthermore, it is readily realized that with increasing experiment time the line intensities will decrease linearly with advancing field because of the transformation of BQ. Increasing the sample volume (*13, 16*) reduces the magnitude of the linear effect as well as of the multiplet effect. In addition, the high initial benzoquinone concentrations favor the TM over the RPM. In a typical experiment, between 10^{-5} and 10^{-4} mol/L of BQ can be excited. Total overall sample volumes are 1 L and initial concentrations vary from 10^{-3} to 2×10^{-2} mol/L. With 1000 laser pulses at 200 field positions, the linear intensity decrease due to depletion is small. The multiplet contribution is, however, visible even when running a 200 s field scan using boxcar time integration with an average of 5000 pulses. At low initial BQ concentrations ($<5 \times 10^{-3}$ mol/L), the multiplet effect contribution is large enough as to make the high field lines appear in absorption while the low field lines are still in emission (cf. Fig. 3c). This effect is not explicable by a mere decrease in intensity due to BQ depletion. Since a multiplet effect was observed at low BQ concentrations even when the sample was not recirculated, it has to be assumed that while setting up the experiment, a sufficient amount of BQH_2 is being formed during the course of the experiment such as to give rise to RPM polarization.

In discussing the influences of the ratio of TM and RPM contributions to the observed polarization, the association–dissociation equilibrium of quinhydrone and the absolute magnitude of the polarizations shall be taken briefly into account. A high BQ concentration ($\sim 10^{-2}$ mol/L) favors quinhydrone formation according to the mass-action law. The overall fraction of hydroquinone and hence quinhydrone is, however, extremely small compared to the larger amount of "free" BQ under the experimental conditions. A weak multiplet effect contribution results. However, at lower BQ concentrations ($\sim 10^{-3}$ mol/L) and assuming a sufficiently strong association tendency, the quantity of quinhydrone becomes nonnegligible during the experiment. As the RPM leads to larger absolute polarization than the TM (*7*), the multiplet contribution becomes more pronounced. As a consequence, the deviation from the theoretical intensity pattern for the dihydroxyethyl radical as expected from TM and shown in Fig. 2a should be interpreted in terms of a decrease in initial BQ concentration, which in turn would lead to fewer solvent radicals. This interpretation is more consistent within the model than invoking a RPM polarization effect due to dissimilar radicals ($\Delta g \neq 0$), which could also account for the high and low field intensity inequalities for the hydroxyalkyl radical. In addition, spectral simulations exhibit far better agreement with a multiplet effect. A striking argument for the existence of two independent pathways of radical creation is provided in Fig. 3d. A solution of hydroquinone with a small amount of benzoquinone clearly shows an intensity distribution for $BQH^{\bullet}$ reflecting a net emission from a TM and a multiplet emission/absorption (E/A) pattern from RPM ($\Delta g = 0$), while no signal originating from the solvent can be detected. This result outlines the appearance of triplet and multiplet polarization from identical molecules, which in this case are most likely benzoquinone and hydroquinone.

CONCLUSION

Benzoquinone, deuterobenzoquinone, and hydroquinone have been investigated in ethylene glycol by means of fast time-resolved EPR spectroscopy. Complete 3-D surfaces representing the magnetization as function of time and external magnetic field have been obtained experimentally for the semiquinones. Based on the Bloch equations, 3-D simulations of the spectral time evolution of benzoquinone system have been achieved. The transient signals unequivocally prove the formation of $BQH^{\bullet}$, d_4-$BQH^{\bullet}$, and 1,2-dihydroxyethyl radicals. The latter exhibits a lifetime of 1.3 μs, which is longer than previously assumed. All radicals observed are found to display emissive TM polarization. In addition, emissive/absorptive contributions from the RPM to the overall polarization of the semiquinones are detected.

More detailed spectral analysis in both time and field domains reveal that the multiplet polarization originating from identical partners exists even at early observation times (100 ns). Hence, two distinct radical generation pathways are assumed: TM polarization is created by reaction of triplet quinone after light excitation and intersystem crossing with ethylene glycol. Independently, multiplet polarization originates from the photochemical reaction between benzoquinone and hydroquinone within the quinhydrone complex, with hydroquinone being formed during the light-induced transformation of benzoquinone. This reaction also leads to additional triplet polarization as a hydrogen atom is formally transferred from BQH_2 to BQ to yield two identical semiquinone molecules. The interpretation thus traces the multiplet effect back to geminate pair polarization (T-pairs). This is in accordance with concentration variation experiments and the observation that a solution of hydroquinone containing small amounts of quinone leads to transient signals characterized by TM and multiplet polarization, but with no hydroxyethyl radicals present in the sample.

ACKNOWLEDGMENTS

MJ and JRN acknowledge support from the U.S. Department of Energy, Office of Basic Energy Sciences, Division of Chemical Sciences Contract DE-FG02-96ER14675. MJ is grateful for a Feodor Lynen Fellowship from the Alexander von Humboldt Association. Helpful discussions with Prof. Hisao Murai are gratefully acknowledged.

REFERENCES

1. L. T. Muus, P. W. Atkins, K. A. McLauchlan, and J. B. Pedersen, Eds. "Chemically Induced Magnetic Polarization," Reidel, Dordrecht, 1977.
2. K. A. McLauchlan, Physical chemistry through electron spin polarisation. The bruker lecture. *J. Chem. Soc. Perkin Trans. II* 2465–2472 (1997).
3. C. M. R. Clancy, V. F. Tarasov, and M. D. E. Forbes, Time-resolved electron paramagnetic resonance studies in organic photochemistry. *Electron Paramagn. Reson.* **16,** 50–78 (1998).
4. N. C. Verma and R. W. Fessenden, Time resolved esr spectroscopy. IV. Detailed measurement and analysis of the esr time profile. *J. Chem. Phys.* **65,** 2139–2155 (1976).
5. M. Plueschau, G. Kroll, K.-P. Dinse, and D. Beckert, Fourier transform electron paramagnetic resonance study of the photoreduction of anthraquinone with 4-methyl-2,6,-di-tert-butylphenol in alcoholic solutions. *J. Phys. Chem.* **96,** 8820–8827 (1992).
6. S. Noda, T. Doba, T. Mizuta, M. Miura, and H. Yoshida, Free radical intermediates in the photoreduction of *p*-benzoquinone in ethanol solution. *J. Chem. Soc. Perkin II* 61–64 (1980).
7. P. J. Hore, C. G. Joslin, and K. A. McLauchlan, Chemically induced dynamic electron polarization. *Chem. Soc. Specialist Period. Rep. ESR* **5,** 1–45 (1979).
8. H. M. Vyas, S. K. Wong, B. B. Adeleke, and J. K. S. Wan, Chemically induced dynamic electron and nuclear polarization in the photolysis of 1,4-benzoquinone in 2-propanol. The radical-pair theory or the photochemical model? *J. Am. Chem. Soc.* **97,** 1385–1387 (1975).
9. S. Patai and Z. Rappoport, Eds. "The Chemistry of Quinoid Compounds," Vol. 1, 2nd ed., Wiley, New York, 1974.
10. J. B. Pedersen, Theory on transient effects in time resolved esr spectroscopy. *J. Chem. Phys.* **59,** 2656–2667 (1973).
11. S. Basu, K. A. McLauchlan, and G. R. Sealy, The continuous wave flash photolysis electron spin resonance spectra of spin-polarized (cidep) radicals using time-integration spectroscopy. *Mol. Phys.* **52,** 431–446 (1984).
12. F. J. Adrian, Theory of anomalous electron spin resonance spectra of free radicals in solution. Role of diffusion-controlled separation and reencounter of radical pairs. *J. Chem. Phys.* **54,** 3918–3923 (1971).
13. J. B. Pedersen, C. E. M. Hansen, H. Parbo, and L. T. Muus, A CIDEP study of *p*-benzosemiquinone. *J. Chem. Phys.* **63,** 2398–2405 (1975).
14. R. W. Eveson and K. A. McLauchlan, Electron spin polarization (CIDEP) studies of the dynamics of geminate free radical reactions. *Mol. Phys.* **96,** 133–142 (1999).
15. M. T. Craw, M. C. Depew, and J. K. S. Wan, A CIDEP study of the photooxidation of benzoquinone in trifluoroacetic acid. *Can. J. Chem.* **64,** 1414–1417 (1986).
16. L. T. Muus, S. Frydkjaer, and K. B. Nielsen, Line dependence of CIDEP polarizations for the *p*-benzosemiquinone radical. *Chem. Phys.* **30,** 163–168 (1978).
17. A. G. Davies, J. A. Howard, M. Lehnig, B. P. Roberts, H. B. Stegmann, and W. Uber, *in* "Landolt-Börnstein. Zahlenwerte und Funktionen aus Naturwissenschaften und Technik," Vol. 9/c2, Springer-Verlag, Berlin, 1979.
18. F. Lendzian, P. Jaegermann, and K. Moebius, Time-resolved CIDEP-enhanced ENDOR on short-lived radicals. *Chem. Phys. Lett.* **120,** 195–200 (1985).
19. A. I. Ononye, A. R. McIntosh, and J. R. Bolton, Mechanism of the photochemistry of *p*-benzoquinone in aqueous solutions. 1. Spin trapping and flash photolysis electron paramagnetic resonance studies. *J. Phys. Chem.* **90,** 6266–6270 (1986).
20. A. I. Ononye and J. R. Bolton, Mechanism of the photochemistry of *p*-benzoquinone in aqueous solutions. 2. Optical flash photolysis studies. *J. Phys. Chem.* **90,** 6270–6274 (1986).
21. J.-C. Ronfard-Haret, R. V. Bensasson, and E. Amouyal, Assignment of transient species observed on laser flash photolysis of *p*-benzoquinone and methylated *p*-benzoquinones in aqueous solution. *J. Chem. Soc. Faraday Trans. I* **76,** 2432–2436 (1980).
22. H.-I. Joschek and S. I. Miller, Photooxidation of phenol, cresols, and dihydroxybenzenes. 2. *J. Am. Chem. Soc.* **88,** 3273–3281 (1966).
23. R. Livingston and H. Zeldes, Paramagnetic resonance study of liquids during photolysis: Hydrogen peroxide and alcohols. *J. Chem. Phys.* **44,** 1245–1259 (1966).
24. L. Monchik and F. J. Adrian, On the theory of chemically induced electron polarization (CIDEP): Vector model and an asymptotic solution. *J. Chem. Phys.* **68,** 4376–4383 (1978).

25. K. A. McLauchlan and M. T. Yeung, On the complete analysis of continuous-wave transient ESR spectra. *Mol. Phys.* **89,** 1423–1443 (1996).

26. C. Blaettler, F. Jent, and H. Paul, A novel radical-triplet pair mechanism for chemically induced electron polarization (CIDEP) of free radicals in solution. *Chem. Phys. Lett.* **166,** 375–380 (1990).

27. G.-H. Goudsmit, H. Paul, and A. I. Shushin, Electron spin polarization in radical-triplet pairs. Size and dependence on diffusion. *J. Phys. Chem.* **97,** 13243–13249 (1993).

28. R. Foster and M. I. Forman, Quinone complexes, *in* "The Chemistry of Quinoid Compounds" (S. Patai and Z. Rappoport, Eds.), Vol. 2, pp. 257–333, Wiley, New York, 1974.